Optics Letters

All optical signal level swapping and multilevel amplitude noise mitigation based on different regions of optical parametric amplification

Yinwen Cao,[1,*] Morteza Ziyadi,[1] Youichi Akasaka,[2] Amirhossein Mohajerin-Ariaei,[1] Jeng-yuan Yang,[2] Ahmed Almaiman,[1] Peicheng Liao,[1] Fatemeh Alishahi,[1] Nisar Ahmed,[1] Asher J. Willner,[1] Shigehiro Takasaka,[3] Ryuichi Sugizaki,[3] Joseph Touch,[1,4] Motoyoshi Sekiya,[2] Moshe Tur,[5] and Alan E. Willner[1]

[1]Department of Electrical Engineering, University of Southern California, Los Angeles, California 90089, USA
[2]Fujitsu Laboratories of America, 2801 Telecom Parkway, Richardson, Texas 75082, USA
[3]Fitel Photonics Laboratories, Furukawa Electric Co., 6 Yawata Kaigan-dori, Ichihara, Chiba 290-8555, Japan
[4]Information Sciences Institute, University of Southern California, Marina del Rey, California 90292, USA
[5]School of Electrical Engineering, Tel Aviv University, Ramat Aviv 69978, Israel
*Corresponding author: yinwenca@usc.edu

Received 9 November 2015; revised 28 December 2015; accepted 5 January 2016; posted 6 January 2016 (Doc. ID 253503); published 4 February 2016

All optical signal level swapping and multilevel amplitude noise mitigation are experimentally demonstrated using the three gain regions of optical parametric amplification, i.e., linear, saturation, and inversion. The two-amplitude-shift-keying and eight-quadrature-amplitude-modulation optical communication systems with baud rates of both 10 and 20 Gbaud have been employed to demonstrate the proposed approaches. Less than 1% error-vector-magnitude degradation is observed after signal level swapping. For amplitude noise mitigation, a more than 20% decrease in amplitude error is confirmed.

OCIS codes: (060.2360) Fiber optics links and subsystems; (060.4370) Nonlinear optics, fibers.

http://dx.doi.org/10.1364/OL.41.000677

Optical signal processing has the potential advantage of fast signal operation, which avoids optoelectronic conversion [1–3]. Typical signal operational functions could be achieved by using the physical properties of optical elements such as a highly nonlinear fiber (HNLF) and a periodically poled lithium niobate (PPLN) waveguide. In the past, nonlinear processes have realized several functions including amplification [4,5], multicasting [6], switching [7,8], and regeneration [9].

Optical parametric amplification (OPA) is a type of nonlinear signal processing [10,11]. Generally, in OPA, an input signal experiences linear gain by power transferred from the pump. However, through a mechanism known as pump depletion [12], a further increase in input signal power would decrease the amplification gain, leading to saturation of the output power. This second gain region (saturation) has been utilized to squeeze amplitude noise for constant-amplitude modulation formats such as quadrature phase-shift keying (QPSK) [13,14]. If the input signal power continues to increase, the gain drops further, and the power is transferred back from the signal to the pump. This results in a third OPA gain inversion region. By using these three different gain regions (linear gain, saturation gain, and gain inversion), specific optical signal processing functions could be achieved [15].

In this Letter, we demonstrate all optical signal level swapping (inversion of amplitude levels) and amplitude noise mitigation for a two-level-amplitude signal. The existence of three OPA gain regions is verified by measuring the gain profile of the OPA in an HNLF. Using only the gain inversion region, signal level swapping is realized for two-amplitude-shift keying (2-ASK) and eight-quadrature-amplitude modulation (8-QAM) with both 10 and 20 Gbaud. A less than 1% error-vector-magnitude (EVM) penalty is observed. In the following, all three gain regions are employed to realize two-level amplitude noise mitigation for 10/20 Gbaud 8-QAM signals within two OPA stages [15]. Furthermore, we experimentally investigate OPA gain profiles under different pump power levels and use the simulation to extend our work of optical amplitude noise mitigation within three OPA stages.

Figure 1(a) explains the three OPA gain regions. Taking a 2-ASK signal as an example, the constellation has two points (A and B) with different amplitude levels. In the linear region, A and B experience the linear OPA gain, while the output constellation and relative waveform remain unchanged. In the saturation region, the input A and B have the same output power. Hence, two constellation points merge into one, and the output waveform has only one level. When the input power level for A and B is even higher, they reach the inversion region. In this case, the output power is inversely related to the input power;

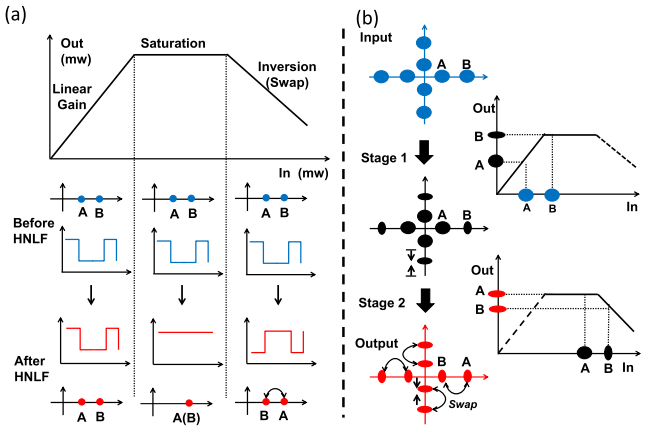

Fig. 1. (a) Three gain regions (linear, saturation, inversion) of OPA. The gain inversion enables signal level swapping: the output amplitude levels are flipped compared with the input. (b) Two-level amplitude noise mitigation. Stage 1, amplitude squeezing for outer circle symbols based on linear and saturation regions; Stage 2, amplitude squeezing for inner circle symbols based on saturation and inversion regions.

therefore, the output constellation points of A and B are exchanged, and the waveform is flipped. This signal level swapping can be effectively employed in multilevel amplitude noise mitigation. It is noted that conventional all optical amplitude noise mitigation, which is usually achieved by OPA saturation, is applicable for a constant-amplitude modulation format such as a QPSK signal [13,14]. This is because amplitude squeezing using OPA gain saturation can be performed only on the highest amplitude level. However, with the help of signal level swapping, the constellation points at the low-amplitude level can be flipped to the high level, and conventional amplitude squeezing can be utilized. Applying this idea to a two-level modulation format such as 8-QAM, all optical amplitude noise mitigation can be achieved [15].

Figure 1(b) shows the concept of two-level amplitude noise mitigation by using all three OPA gain regions. The input is an 8-QAM signal degraded by amplified spontaneous emission (ASE) noise. At Stage 1, by changing the signal power, the noisy symbols at the upper level reach the OPA saturation region, while the noisy symbols at the lower level fall into the OPA linear region. In this case, the noise on the upper level symbols is squeezed, while the noise on the lower level symbols stays the same, as shown in Fig. 1(b). At Stage 2, by tuning the signal power, the upper level symbols reach the inversion gain region, and the lower level symbols fall into the saturation region. At the output, not only are the symbol levels swapped, but the noise on the lower level symbols is also squeezed. Therefore, by utilizing the three OPA gain regions, the amplitude of the noise on both of the two levels is squeezed. It is noted that since the amplitude levels of the final output are flipped compared with the original input signal, another swapping stage might be needed to recover the original constellation.

Figure 2 illustrates the experimental setup for the measurement of OPA gain regions and all optical signal level swapping. To measure the gain profile, a continuous wave (CW) signal at 1560 nm is coupled with a pump at 1556.3 nm. To suppress the stimulated Brillouin scattering (SBS) effect, both the CW and pump are phase modulated. For the gain profile measurement, the module of ASK modulation is bypassed. Then, the signal

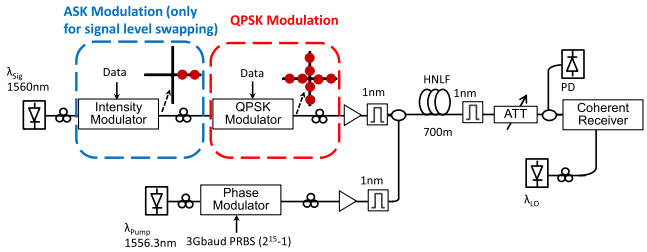

Fig. 2. Experimental setup for the OPA characterization (without 2-ASK signal modulation) and signal level swapping (with 2-ASK signal modulation). PRBS: pseudorandom binary sequence; ATT: attenuator; PD: photodiode.

and pump are coupled in a 700 m HNLF with a nonlinear coefficient of 21.4 W^{-1} km^{-1}, a zero dispersion wavelength (ZDW) of 1551.5 nm, and a dispersion slope of 0.043 ps/km/nm^2. The OPA gain profile is characterized by varying the power of the input signal.

Figure 3(a) depicts the relationship between signal input power and signal output power after OPA. When the pump power is 1 W, with increasing signal input power, the signal output power grows linearly with 9 dB gain. As the input power exceeds 12 dBm, the OPA gain decreases, but the output power still grows. This gain profile cannot be utilized for signal level swapping. When the pump power is increased to be at least 1.5 W, as shown in Fig. 3(a), the signal output power first similarly experiences constant OPA gain, then grows slower and becomes saturated. Furthermore, when signal input power continues to increase, the output power begins to drop.

The gain profiles under different pump powers are in Fig. 3(b). Besides the sharp drops in the gain curves for pump powers of 1.5 and 2 W, the gain can also be negative, as shown within the dashed circle, which is a unique property of HNLFs compared with erbium-doped fiber amplifiers (EDFA). This is due to the power of the signal being transferred to the pump, as well as to the other high-order harmonics. In the region between two dashed lines in Fig. 3(a), amplitude squeezing and signal swapping can be realized simultaneously if the lower level input symbols reach the flat region (gain saturation) and the upper level input symbols reach the descending region (gain inversion).

Two-amplitude-level modulation formats such as 2-ASK and 8-QAM are employed to evaluate all optical signal level swapping. In Fig. 2, the 8-QAM signal is emulated by modulating data with a 2-ASK signal followed by a QPSK

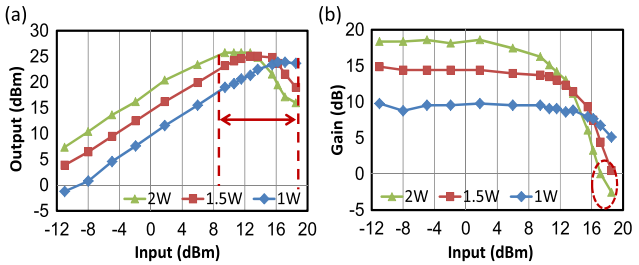

Fig. 3. (a) Measured input–output curves with different pump powers (1, 1.5, and 2 W). Both saturation and inversion OPA regions are observed with 1.5 and 2 W pumps. (b) Gain profiles.

modulator. The signal power and pump power are set to be 0.15 W and 1.5 W, respectively. At the receiver side, the signal is split into two paths. In one path, a photodiode (PD) is used to record the waveform, while in the other path, coherent detection is utilized to obtain the constellation and evaluate the signal quality.

Figure 4(a) shows the waveform of a 10 Gbaud 8-QAM signal at the input and output. The inverted waveform indicates successful signal level swapping. Similar waveform inversion has been observed for a 20 Gbaud 8-QAM signal in Fig. 4(b).

The EVMs of the input and output signals are compared in Fig. 5. Less than 1% EVM increase at the output indicates the preservation of signal quality after the operation. It is noted that the EDFA power for the signal should be carefully tuned to ensure that its two distinct power levels reach the suitable OPA regions to have the optimal swapping performance.

Figure 6(a) is the experimental setup for amplitude noise mitigation of an 8-QAM signal. The signal is degraded by an ASE source at the transmitter. Stage 1 is used for amplitude noise squeezing of the high level symbols, where an 8-QAM signal with a power of 0.12 W is coupled with a 2 W pump in the 900 m HNLF-1 with a ZDW of 1556 nm and a

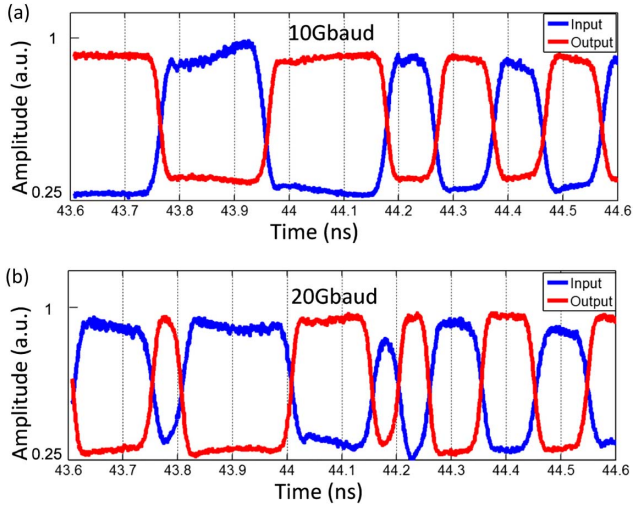

Fig. 4. Experimental demonstration of signal level swapping for different baud rates: (a) waveform flipping for 10 Gbaud 8-QAM signal and (b) waveform flipping for 20 Gbaud 8-QAM signal. It is noted that both the input and output measurements are normalized.

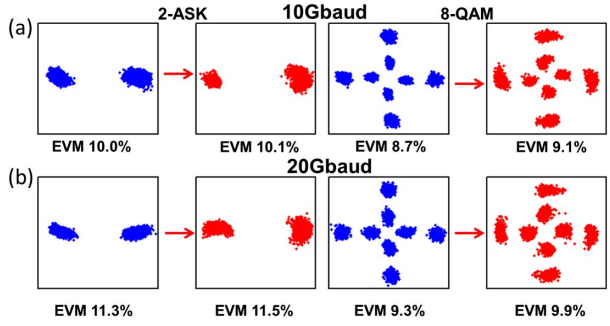

Fig. 5. Constellation EVM comparison before and after all optical signal level swapping: (a) 10 Gbaud 2-ASK/8-QAM and (b) 20 Gbaud 2-ASK/8-QAM. EVM degradation is less than 1%.

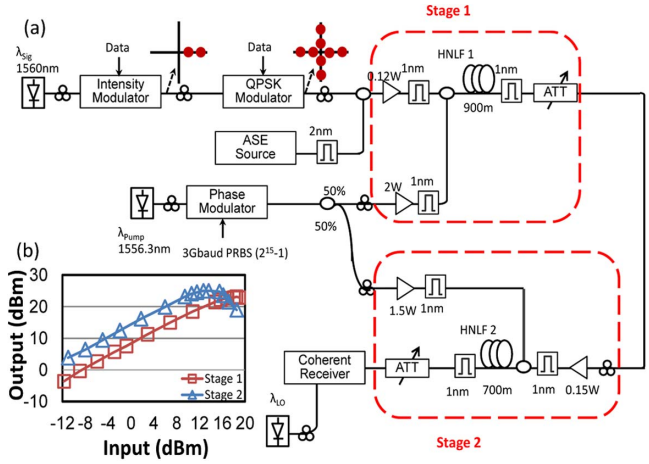

Fig. 6. (a) Experimental setup for amplitude noise mitigation of 10/20 Gbaud 8-QAM signals. Stage 1 is for upper level amplitude noise mitigation, and Stage 2 is for lower level amplitude noise mitigation. (b) Input and output power profiles for HNLF-1 (square symbols) and HNLF-2 (triangle symbols).

nonlinear coefficient of 9.2 W^{-1} km^{-1}. The characteristics of HNLF-1 are measured with the same method described in Fig. 2. The input and output power profile is shown in Fig. 6(b) with square symbols. The saturation region occurs when the power level exceeds 16 dBm. In Stage 2, the signal is coupled with a divided pump source of 1.5 W in the 700 m HNLF-2 with the same characteristics in Fig. 3. The input and output power profile is also depicted in Fig. 6(b) with triangle symbols. Here, signal level swapping and amplitude squeezing are simultaneously achieved. Compared with the power profile of HNLF-1, for the same input power, the gain of HNLF-2 is nearly 6 dB higher, and both saturation and inversion regions are observed. This is due to the fact that HNLF-2 has a much higher nonlinear coefficient.

By adding ASE noise on the original signal, the constellation diagram is scattered in Figs. 7(a) and 7(b). After Stage 1, the upper level symbols are squeezed. As a result, the amplitude error, defined as the root mean square (RMS) of the amplitude difference between the received and ideal constellations, is decreased from 8.26% to 7.07% and 9.7% to 8.2% for 10 Gbaud and 20 Gbaud signals, respectively, in Fig. 7(c). After Stage 2, it can be seen in Fig. 7(c) that the amplitude error is decreased further to 5.98% and 7.74%, respectively. The total decrease in amplitude error is more than 20%. However, due to the high power of the system, the additional nonlinear phase noise leads to the EVM degradation in Fig. 7(c). Although the degraded

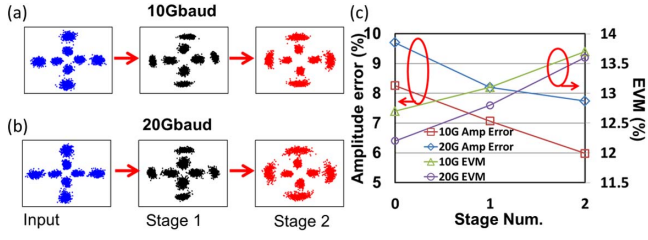

Fig. 7. (a) 10 Gbaud and (b) 20 Gbaud 8-QAM constellations after each stage for two-level amplitude noise mitigation. (c) Measured amplitude error and EVM comparison after each stage.

EVM would increase the bit error rate (BER), this system penalty might be compensated by other phase squeezing approaches [14,16,17].

Because there are only two stages in the above experiment, the levels of the output signal are flipped, which can be corrected in the electrical domain at the receiver. To investigate the complete process of optical amplitude noise mitigation, one more stage is required for a final optical signal level swapping. Figure 8 depicts the simulation for the amplitude noise mitigation of an 8-QAM signal with three OPA stages. 28 Gbaud 8-QAM data are generated by an in-phase and quadrature (IQ) modulator at the transmitter. The 200 m HNLFs in all three stages have the same nonlinear index of 9.1e – 20 m^2/W, and the three pumps have the same power of 31 dBm. The necessary change for the signal power is realized by tuning the attenuators at the input of each stage.

Figure 9 shows the simulation performance. The input signal degraded by ASE is shown in Fig. 9(a). Figure 9(b) is the final output. The constellation diagram shows that the amplitude noise is effectively suppressed. The similar output waveform compared to the input indicates the signal is flipped back.

The current approach is based on two-level-amplitude modulation formats. If more cascading stages are available, amplitude noise mitigation for higher level modulations such as 16-QAM might be achieved. On the other hand, if a three-level staircase amplitude quantization similar to [9] could potentially be constructed, the amplitude squeezing of 16-QAM might be simplified with one stage.

The problem of high power consumption in this approach typically might be alleviated by using HNLFs with higher nonlinearity or a longer length. Meanwhile, the additional nonlinear phase noise could be mitigated by several approaches [14,16,17]. Also, extension of a wavelength-division multiplexing (WDM) application can be supported by the recently fabricated dispersion stable HNLF with a ~50 nm flat OPA gain region [18]. Although the cross talk from four-wave mixing (FWM) between different channels degrades system performance, it could be mitigated by other methods such as unequal channel spacing [19] and polarization interleaving [20]. Furthermore, if WDM is implemented, smaller input power on a single channel might be enough for OPA saturation and inversion, which is potentially helpful in reducing the power consumption per channel and the nonlinear phase noise.

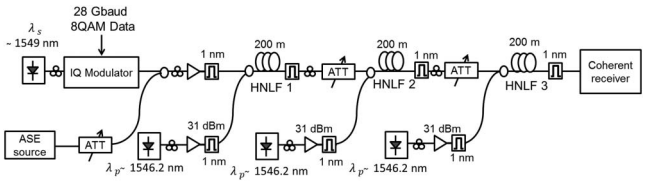

Fig. 8. Simulation setup for amplitude noise mitigation of 28 Gbaud 8-QAM signal using three cascaded OPA stages.

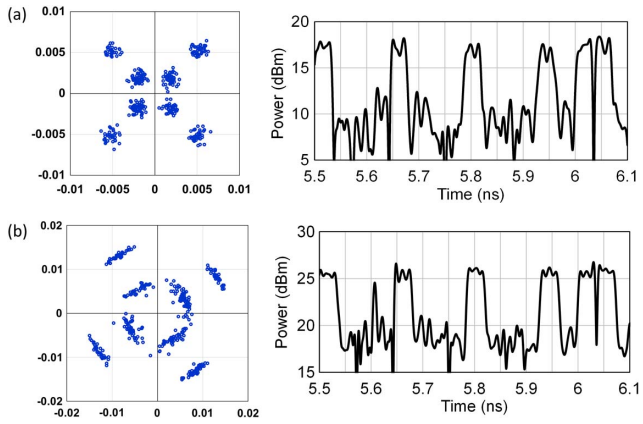

Fig. 9. Constellations and waveforms comparison of 28 Gbaud 8-QAM signal (a) before and (b) after amplitude noise mitigation.

Funding. Center for Integrated Access Network (CIAN); National Science Foundation (NSF).

REFERENCES

1. M. Saruwatari, IEEE J. Sel. Top. Quantum Electron. **6**, 1363 (2000).
2. A. E. Willner, S. Khaleghi, M. Chitgarha, and O. Yilmaz, J. Lightwave Technol. **32**, 660 (2014).
3. R. Slavík, F. Parmigiani, J. Kakande, C. Lundström, M. Sjödin, P. Andrekson, R. Weerasuriya, S. Sygletos, A. Ellis, L. Nielsen, D. Jakobsen, S. Herstrøm, R. Phelan, J. O'Gorman, A. Bogris, D. Syvridis, S. Dasgupta, P. Petropoulos, and D. Richardson, Nat. Photonics **4**, 690 (2010).
4. T. Umeki, H. Takara, Y. Miyamoto, and M. Asobe, Opt. Express **20**, 24727 (2012).
5. K. J. Lee, F. Parmigiani, S. Liu, J. Kakande, P. Petropoulos, K. Gallo, and D. Richardson, Opt. Express **17**, 20393 (2009).
6. G. Lu, T. Sakamoto, and T. Kawanishi, in *Optical Fiber Communication Conference (OFC)* (Optical Society of America, 2015), paper M2E.2.
7. H. Hu, E. Palushani, M. Galili, H. Mulvad, A. Clausen, L. Oxenløwe, and P. Jeppesen, Opt. Express **18**, 9961 (2010).
8. J. Leuthold, L. Moller, J. Jaques, S. Cabot, L. Zhang, P. Bernasconi, M. Cappuzzo, L. Gomez, E. Laskowski, E. Chen, A. Wong-Foy, and A. Griffin, Electron. Lett. **40**, 554 (2004).
9. J. Kakande, R. Slavík, F. Parmigiani, A. Bogris, D. Syvridis, L. Nielsen, R. Phelan, P. Petropoulos, and D. Richardson, Nat. Photonics **5**, 748 (2011).
10. J. Hansryd and P. Andrekson, IEEE Photon. Technol. Lett. **13**, 194 (2001).
11. P. Kylemark, P. Hedekvist, H. Sunnerud, M. Karlsson, and P. Andrekson, J. Lightwave Technol. **22**, 409 (2004).
12. M. Marhic, K. Wong, M. Ho, and L. Kazovsky, Opt. Lett. **26**, 620 (2001).
13. X. Guo, K. Lei, X. Fu, H. Tsang, and C. Shu, in *Optical Fiber Communication Conference (OFC)* (Optical Society of America, 2013), paper OTu2D.
14. F. Parmigiani, K. R. H. Bottrill, L. Jones, G. Hesketh, D. J. Richardson, and P. Petropoulos, in *European Conference on Optical Communication (ECOC)* (2015), paper We.3.6.3.
15. Y. Cao, M. Ziyadi, Y. Akasaka, A. Mohajerin-Ariaei, J. Yang, A. Almaiman, P. Liao, S. Takasaka, R. Sugizaki, J. Touch, M. Sekiya, M. Tur, and A. Willner, in *Optical Fiber Communication Conference (OFC)* (Optical Society of America, 2015), paper W2A.49.
16. B. Stiller, G. Onishchukov, B. Schmauss, and G. Leuchs, Opt. Express **22**, 1028 (2014).
17. J. Yang, Y. Akasaka, and M. Sekiya, in *European Conference on Optical Communication (ECOC)* (2012), paper P3.07.
18. S. Takasaka, Y. Taniguchi, M. Takahashi, J. Hiroshi, M. Tadakuma, H. Matsuura, K. Doi, and R. Sugizaki, in *Optical Fiber Communication Conference (OFC)* (Optical Society of America, 2014), paper W3E.2.
19. F. Forghieri, R. W. Tkach, A. R. Chraplyvy, and D. Marcuse, IEEE Photon. Technol. Lett. **6**, 754 (1994).
20. K. K. Y. Wong, G.-W. Lu, and L.-K. Chen, Opt. Express **15**, 56 (2007).